

This is the accepted manuscript made available via CHORUS, the article has been published as:

## Vector boson fusion processes as a probe of supersymmetric electroweak sectors at the LHC

Bhaskar Dutta, Alfredo Gurrola, Will Johns, Teruki Kamon, Paul Sheldon, and Kuver Sinha

Phys. Rev. D **87**, 035029 — Published 22 February 2013

DOI: [10.1103/PhysRevD.87.035029](https://doi.org/10.1103/PhysRevD.87.035029)

# Vector Boson Fusion Processes as a Probe of Supersymmetric Electroweak Sectors at the LHC

Bhaskar Dutta<sup>1</sup>, Alfredo Gurrola<sup>2</sup>, Will Johns<sup>2</sup>, Teruki Kamon<sup>1,3</sup>, Paul Sheldon<sup>2</sup>, and Kuver Sinha<sup>1</sup>

<sup>1</sup> *Mitchell Institute for Fundamental Physics and Astronomy,*

*Department of Physics, Texas A&M University, College Station, TX 77843-4242, USA*

<sup>2</sup> *Department of Physics and Astronomy, Vanderbilt University, Nashville, TN, 37235*

<sup>3</sup> *Department of Physics, Kyungpook National University, Daegu 702-701, South Korea*

Vector boson fusion (VBF) processes offer a promising avenue to study the non-colored sectors of supersymmetric extensions of the Standard Model at the LHC. A feasibility study for searching for the chargino/neutralino system in the  $R$ -parity conserving Minimal Supersymmetric Standard Model is presented. The high  $E_T$  forward jets in opposite hemispheres are utilized to trigger VBF events, so that the production of the lightest chargino  $\tilde{\chi}_1^\pm$  and the second lightest neutralino  $\tilde{\chi}_2^0$  can be probed without a bias by experimental triggers. Kinematic requirements are developed to search for signals of these supersymmetric states above Standard Model backgrounds in both  $\tau$  and light lepton ( $e$  and  $\mu$ ) final states at  $\sqrt{s} = 8$  TeV.

## I. INTRODUCTION

The LHC has put bounds on the masses of the gluino ( $\tilde{g}$ ) and first two generation squarks ( $\tilde{q}$ ). For comparable masses, they are excluded up to about 1500 GeV at 95% CL at  $\sqrt{s} = 7$  TeV with  $4.7 \text{ fb}^{-1}$  of integrated luminosity [1–3]. Limits on the masses of the third generation colored superpartners have also been under serious theoretical scrutiny recently [4, 5], and bounds in certain decay modes have been obtained from the LHC [6].

On the other hand, the bounds on charginos and neutralinos are less constrained, since, expectedly, these particles suffer from smaller electroweak (EW) production in a hadron collider. The chargino/neutralino system plays a crucial role in the dark matter connection of supersymmetric models. The lightest neutralino  $\tilde{\chi}_1^0$ , as the lightest supersymmetric particle (LSP), is the canonical dark matter candidate in the  $R$ -parity conserving minimal supersymmetric extension of the Standard Model (MSSM). Various schemes of supersymmetry breaking and mediation predict  $m_{\tilde{\chi}_2^0}$  (where  $\tilde{\chi}_2^0$  is the second lightest neutralino) and  $m_{\tilde{\chi}_1^\pm}$  (where  $\tilde{\chi}_1^\pm$  is the lightest chargino) to be larger by a factor of 1 – 3 than  $m_{\tilde{\chi}_1^0}$ , under broad assumptions [7]. For Higgsino-like  $\tilde{\chi}_1^0$ , the degeneracy is much stronger [8]. This implies that if  $m_{\tilde{\chi}_1^0}$  is in the mass range of  $\mathcal{O}(100)$  GeV, the  $\tilde{\chi}_2^0, \tilde{\chi}_1^\pm$  system may be expected to be in the 100 – 300 GeV range, which is within the range of detection at the LHC given suitable search strategies.

From the perspective of a hadron collider, where EW production is small, a classic strategy to study the chargino/neutralino system is to detect the neutralinos in cascade decays of gluinos and squarks. For example, reconstructing a decay chain like  $\tilde{g} \rightarrow \tilde{q} \rightarrow \tilde{\chi}_2^0 \rightarrow \tilde{\tau}_1 \rightarrow \tilde{\chi}_1^0$  using endpoint methods [9, 10] leads to mass measurements of  $\tilde{\chi}_2^0, \tilde{\tau}_1, \tilde{q}$  and  $\tilde{g}$ , where  $\tilde{\tau}_1$  is the lighter stau mass [11]. However, in a scenario where colored objects are heavy and the production cross-section is limited, one

has to use different techniques to probe the EW sector.

The purpose of this paper is to show that the chargino/neutralino system can be studied in events through vector boson fusion (VBF) processes [12, 13]. VBF processes have been suggested for Higgs searches [14] and supersymmetric searches, in the context of slepton and gaugino productions at 14 TeV LHC [15–17]. VBF production is characterized by the presence of two jets with large dijet invariant mass in the forward region in opposite hemispheres. A sample diagram of chargino production from VBF processes is shown in Figure 1.

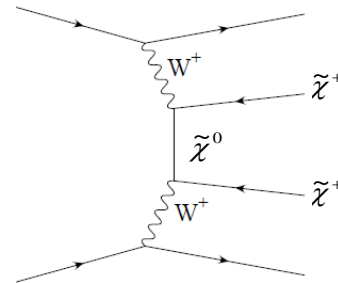


FIG. 1: Feynman diagram of production of charginos pairs by VBF processes.

Direct searches for  $\tilde{\chi}_2^0$  and  $\tilde{\chi}_1^\pm$  at ATLAS [18, 19] and CMS [20] mainly involve the search for signal in events with 3 leptons and  $\cancel{E}_T$ :  $\tilde{\chi}_1^\pm \tilde{\chi}_2^0 \rightarrow ll\ell\nu\tilde{\chi}_1^0\tilde{\chi}_1^0$ <sup>1</sup>. This

<sup>1</sup> For example, ATLAS bounds in the trilepton +  $\cancel{E}_T$  searches at  $\sqrt{s} = 7$  TeV, with  $4.7 \text{ fb}^{-1}$  of integrated luminosity rule out charginos with mass up to about 500 GeV for  $m_{\tilde{\chi}_1^0} < 230$  GeV and large branching ratios of  $\tilde{\chi}_1^\pm$  and  $\tilde{\chi}_2^0$  to a slepton. In anomaly-mediated supersymmetry breaking scenarios, ATLAS has placed a bound on the chargino mass of 90 GeV, for  $m_{3/2} < 32$  TeV,  $m_0 < 1.5$  TeV,  $\tan\beta = 5$  and  $\mu > 0$ .

can proceed through  $\tilde{\chi}_1^\pm$  decaying through  $(\tilde{\nu}l)$ ,  $(\tilde{l}_1\nu)$ , or  $(W^{\pm(*)}\tilde{\chi}_1^0)$ , and  $\tilde{\chi}_2^0$  decaying to  $(\tilde{l}_1l)$ ,  $(\tilde{\nu}\nu)$ , or  $(Z^{(*)}\tilde{\chi}_1^0)$ .

Several features of existing searches at the LHC may be highlighted for better contrast with the present study:

(a) Searches target  $\tilde{\chi}_2^0$  and  $\tilde{\chi}_1^\pm$  produced via Drell-Yan production, i.e., without requiring the presence of forward/backward jets.

(b) The bounds assume  $m_{\tilde{\chi}_1^\pm} \sim m_{\tilde{\chi}_2^0}$  and an enhanced branching ratio to trilepton final state provided by  $m_{\tilde{l}_1} \sim (m_{\tilde{\chi}_1^\pm} + m_{\tilde{\chi}_1^0})/2$  (where  $\tilde{l}_1$  is the lighter slepton, and  $l$  denotes either  $e$  or  $\mu$ ). The slepton mass  $m_{\tilde{l}_1}$  is carefully placed such that the mass splitting is large and thus the leptons have relatively high  $p_T$  to be free from trigger bias.

(c) Searches resulting in  $\tau$  final states do not exist due to the larger  $\tau$  misidentification rates which make it difficult to both manage the level of backgrounds and maintain low enough  $p_T$  thresholds for triggering.

In this paper, final states with  $2\tau + \cancel{E}_T$  as well as  $2l + \cancel{E}_T$  (along with two high  $p_T$  forward/backward jets) arising from  $\tilde{\chi}_1^\pm$  and  $\tilde{\chi}_2^0$  produced by VBF processes are studied. This offers certain advantages:

(i) With increasing instantaneous luminosity at the LHC, both ATLAS and CMS experiments are raising their  $p_T$  thresholds for triggering any object. This motivates us to probe signals for supersymmetry in VBF processes at  $\sqrt{s} = 8$  TeV where production of superpartners in VBF processes are free from trigger bias.

(ii) VBF production allows the investigation of final states with  $\tau$ .  $\tilde{\tau}_1$  is typically lighter than  $\tilde{\mu}_1$  and  $\tilde{e}_1$  for large  $\tan\beta$ . A light  $\tilde{\tau}_1$  with small mass splitting is favored in coannihilation processes [21] that set the relic density to correct values, in the case of Bino dark matter. Light  $\tilde{\tau}_1$  is also motivated in the context of the MSSM by the enhancement of the  $h \rightarrow \gamma\gamma$  channel [22]. These facts stress the importance of searches in  $\tau$  final states with low  $p_T$  and large backgrounds, for which production by VBF processes is more suited since the VBF signature allows for the reduction of the backgrounds to manageable levels.

(iii) For the leptonic final state, a search based on VBF processes can be complementary or better than the existing LHC searches based on Drell-Yan production, since it is not constrained by the trigger bias. It is also interesting to note that the Drell-Yan production cross-section falls faster than the VBF production cross-section with increasing mass [15].

The structure of the paper is as follows. In Section II an outline of the search strategy is given, followed by results in Section III. Conclusions are given in Section IV.

## II. SEARCH STRATEGY

The  $\tilde{\chi}_2^0$  and  $\tilde{\chi}_1^\pm$  are produced by VBF processes and then decay into the lighter slepton states ( $\tilde{\tau}_1$ ,  $\tilde{\mu}_1$  and  $\tilde{e}_1$ )

by the decay processes  $\tilde{\chi}_1^\pm \rightarrow \tilde{\tau}_1\nu \rightarrow \tilde{\chi}_1^0\tau\nu$ ,  $\tilde{\chi}_1^\pm \rightarrow \tilde{l}_1\nu \rightarrow \tilde{\chi}_1^0l\nu$ , and similarly for  $\tilde{\chi}_2^0$  via  $\tilde{\chi}_2^0 \rightarrow \tilde{\tau}_1\tau \rightarrow \tilde{\chi}_1^0\tau\tau$  and  $\tilde{\chi}_2^0 \rightarrow \tilde{l}_1l \rightarrow \tilde{\chi}_1^0ll$ .

Depending on the branching ratio of  $\tilde{\chi}_2^0$  and  $\tilde{\chi}_1^\pm$  to  $\tilde{l}$  and  $\tilde{\tau}_1$  the results presented here can be used in feasibility studies of detecting different models with smaller chargino/neutralino masses around the EW scale at the LHC.

A benchmark point is first defined and the following processes are investigated:

$$pp \rightarrow \tilde{\chi}_1^\pm \tilde{\chi}_1^\pm jj, \tilde{\chi}_1^\pm \tilde{\chi}_1^\mp jj, \tilde{\chi}_1^\pm \tilde{\chi}_2^0 jj, \tilde{\chi}_2^0 \tilde{\chi}_2^0 jj. \quad (1)$$

The benchmark point is  $m_{\tilde{\chi}_1^\pm} \sim m_{\tilde{\chi}_2^0} = 181$  GeV,  $m_{\tilde{\tau}_1} = 130$  GeV, and  $m_{\tilde{\chi}_1^0} = 100$  GeV. The  $\tilde{\chi}_1^\pm$  and  $\tilde{\chi}_2^0$  are mainly Wino, while  $\tilde{\chi}_1^0$  is mainly Bino.

The search strategy is based on two steps: first, use the unique features of VBF processes to reduce background  $V$ +jets events (where  $V$  is either  $W$  or  $Z$ ), and second, use decay properties of the centrally produced supersymmetric particle to reduce non-supersymmetric channels that are also produced by VBF processes.

(1) VBF processes: VBF processes are characterised by the production of two energetic jets produced in the forward-backward regions with large  $|\Delta\eta|$ . Requirements on  $|\Delta\eta|$  as well as  $M_{jj}$ , where  $M_{jj}$  is the dijet invariant mass, are effective in reducing  $V$ +jets and  $t\bar{t}$  background events, where the jets are less energetic and more central. Moreover, the leading jet is expected to have high  $p_T$  since the incoming partons need significant momentum to create a pair of heavy supersymmetric states. This motivates a  $p_T$  cut on the leading jet to reduce background.

(2) Decay of  $\tilde{\chi}_1^\pm$  and  $\tilde{\chi}_2^0$ : Having reduced the background using the above selections, the remnant background consists of other particles that have been produced centrally, also by VBF processes. For  $R$ -parity conserving models, the decay of the charginos and neutralino proceeds as

$$\begin{aligned} \tilde{\chi}_1^\pm &\rightarrow \tilde{\tau}_1^\pm \nu \rightarrow \tau^\pm \tilde{\chi}_1^0 \nu \\ \tilde{\chi}_2^0 &\rightarrow \tilde{\tau}_1^\pm \tau^\mp \rightarrow \tau^\pm \tau^\mp \tilde{\chi}_1^0. \end{aligned} \quad (2)$$

The  $\tilde{\chi}_1^0$  LSP escapes the detector as the dark matter candidate, and gives rise to  $\cancel{E}_T$ .

The production of  $VV$  (where  $V$  may be either  $W$  or  $Z$ ) by VBF processes mimics the signal when the bosons decay leptonically. A  $\cancel{E}_T$  cut is effective in reducing this background. Moreover, requiring multiple  $\tau$ 's in the event further reduces background. Results will be presented for requiring same-sign and oppositely-signed  $\tau$  pairs, as well as an inclusive study. Although  $m_{\tilde{\chi}_1^\pm} \sim m_{\tilde{\chi}_2^0}$  is chosen as an example, the methods described in this paper are applicable in detecting  $\tilde{\chi}_2^0$  and  $\tilde{\chi}_1^\pm$  separately.

After presenting results in the  $2\tau$  event selection, further results will be presented for  $2l$  event selection, corresponding to

$$\tilde{\chi}_2^0 \rightarrow \tilde{l}_1^\pm l^\mp \rightarrow l^\pm l^\mp \tilde{\chi}_1^0. \quad (3)$$

### III. RESULTS

In this section, the main results are presented. Signal and background samples are generated with Madgraph [23] followed by detector simulation using PGS4 [24].

For the VBF selections, motivated in the search strategy in Section II, we accept jets with  $p_T \geq 50$  GeV in  $|\eta| \leq 5$ , and require a presence of two jets ( $j_1, j_2$ ) satisfying:

- (i)  $p_T(j_1) \geq 75$  GeV;
- (ii)  $|\Delta\eta(j_1, j_2)| > 4.2$ ;
- (iii)  $\eta_{j_1}\eta_{j_2} < 0$ ;
- (iv)  $M_{j_1 j_2} > 650$  GeV.

We note that the signal acceptance with this selection is less sensitive to effects on the signal acceptance due to initial/final state radiation, pileup, and fluctuations in jet fragmentation.

The production cross-sections at  $\sqrt{s} = 8$  TeV for  $\tilde{\chi}_1^\pm \tilde{\chi}_1^\pm$ ,  $\tilde{\chi}_1^\pm \tilde{\chi}_1^\mp$ ,  $\tilde{\chi}_1^\pm \tilde{\chi}_2^0$ , and  $\tilde{\chi}_2^0 \tilde{\chi}_2^0$  as a function of mass after imposing just  $|\Delta\eta| > 4.2$  are displayed in Figure 2. For the  $\tilde{\chi}_1^\pm \tilde{\chi}_1^\pm$  mode, the production cross-section is  $\sim 7$  fb for  $m_{\tilde{\chi}_1^\pm} \sim 100$  GeV, while for oppositely signed charginos, the corresponding cross-section is  $\sim 5$  fb. At the benchmark value of  $m_{\tilde{\chi}_1^\pm} = 181$  GeV, the corresponding values are 2.5 fb and 1.5 fb respectively. We have used Madgraph 4 for our calculation.

The appreciable production cross-sections for  $\tilde{\chi}_1^\pm \tilde{\chi}_1^\pm$  and  $\tilde{\chi}_1^\pm \tilde{\chi}_2^0$  mean that same-sign  $\tau$ 's are significantly present in the final state. As will be seen, the same-sign  $\tau$  selection leads to considerable reduction of background.

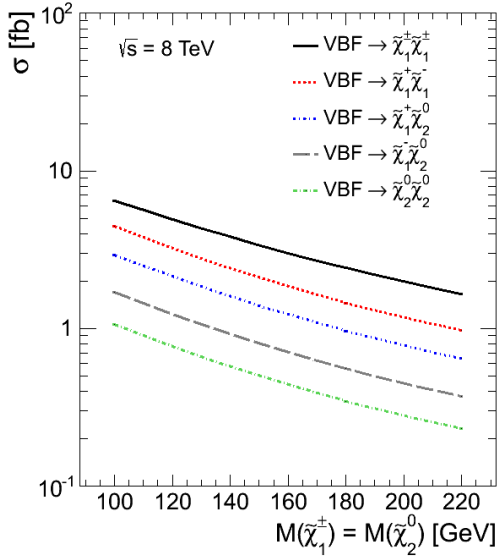


FIG. 2: VBF production cross-section at  $\sqrt{s} = 8$  TeV as a function of mass for various channels after imposing  $|\Delta\eta| > 4.2$  using Madgraph 4.

In Figures 3 and 4, the distributions of  $M_{j_1 j_2}$  and the  $p_T$  of the leading jet are displayed for  $\tilde{\chi}_1^\pm \tilde{\chi}_1^\pm$  pair pro-

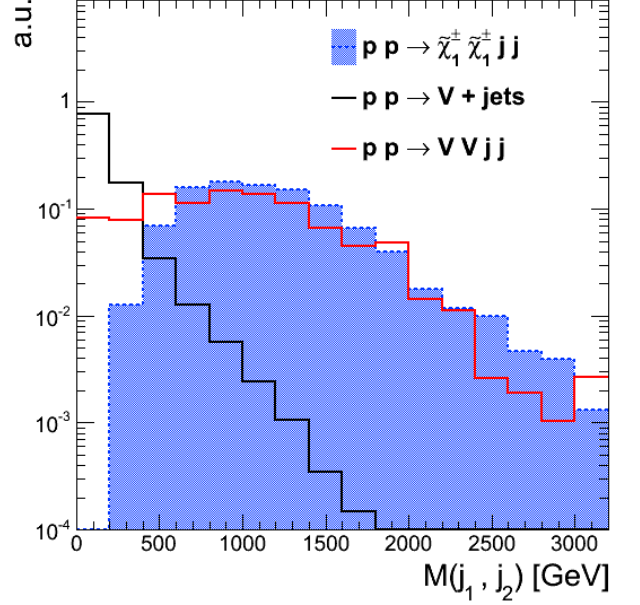


FIG. 3:  $M_{j_1 j_2}$  distribution normalized to arbitrary units for  $\tilde{\chi}_1^\pm \tilde{\chi}_1^\pm$  pair production by VBF processes, V+jets background, and VV background produced by VBF processes.

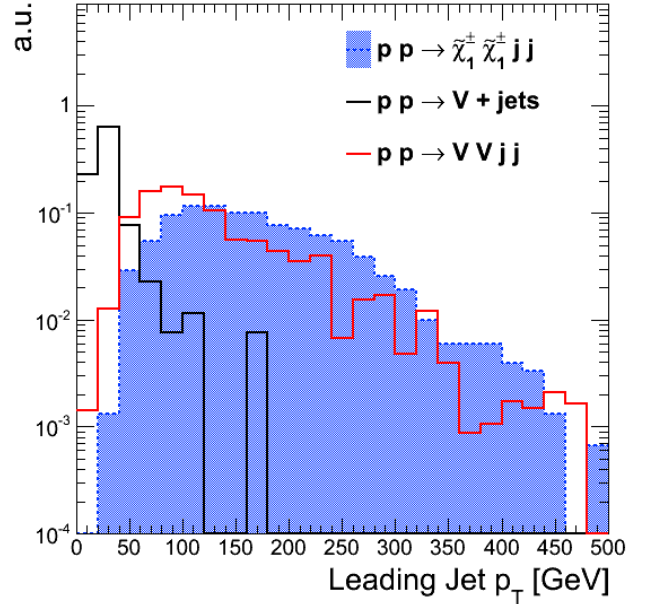


FIG. 4:  $p_T$  distribution of the leading jet normalized to arbitrary units for  $\tilde{\chi}_1^\pm \tilde{\chi}_1^\pm$  pair production by VBF processes, V+jets background, and VV background produced by VBF processes.

duction by VBF processes, V+jets background, and VV background produced by VBF processes. The VBF production channels have large  $M_{j_1 j_2}$  due to the highly energetic forward jets. The leading jet has high  $p_T$  required

to create a pair of heavy supersymmetric states. The VBF selections are thus very effective in reducing the background.

Although the central jet veto has been used in the past for VBF Higgs, we do not employ a central veto cut in our case as our backgrounds are already small and such a veto in high pileup conditions can degrade the signal acceptance and requires extensive study in the future.

We reviewed a successful CMS analysis of forward/backward jets along with  $Z$  production at 7 TeV [25], which demonstrated the powerful and efficient identification of forward/backward jets. Furthermore, we do not foresee any problems carrying out any CMS analysis with 8 TeV. For example,  $\cancel{E}_T$  is calculated using the entire detector (calorimeter coverage up to  $|\eta| = 5$ ). The same conclusion holds for ATLAS [26]. Thus, we expect that both ATLAS and CMS will be able to carry out these VBF analyses at 8 TeV.

With our proposed VBF cuts, it is fruitful to divide the study into the  $2\tau + \cancel{E}_T$  and  $2l + \cancel{E}_T$  final states separately.

#### A. $\geq 2j + 2\tau + \cancel{E}_T$

For this final state, the following selections are employed in addition to the VBF cuts described above:

(i) Two  $\tau$ 's with  $p_T \geq 20$  GeV in  $|\eta| < 2.1$ , with  $\Delta R(\tau, \tau) > 0.3$ . All  $\tau$ 's considered in this paper are hadronic. The  $\tau$  ID efficiency is assumed to be 55% and the jet  $\rightarrow \tau$  misidentification rate is taken to be 1%, both flat over  $p_T$  [27]. A branching ratio of 100% of  $\tilde{\chi}_1^\pm$  and  $\tilde{\chi}_2^0$  to  $\tilde{\tau}_1$  has been assumed. In realistic models, this branching ratio can be close to 100%.

(ii)  $\cancel{E}_T > 75$  GeV. This cut is expected to be effective, due to the fact that the main source of  $\cancel{E}_T$  for signal is the  $\tilde{\chi}_1^0$  LSP which leaves the detector, while for the background it is the neutrinos produced by leptonic decays of the vector bosons.

(iii) We also apply a loose  $b$ -veto which is useful in reducing the  $t\bar{t}$  background.

In Figure 5, the normalized distribution of the  $p_T$  of  $\tau$  is displayed for  $\Delta M = m_{\tilde{\chi}_1^\pm} - m_{\tilde{\chi}_1^0} = 30$  GeV and 15 GeV. For smaller  $\Delta M$ , the distribution peaks at lower  $p_T$  and the signal acceptance is less efficient.

In Figure 6, the  $\cancel{E}_T$  distribution is displayed for  $\tilde{\chi}_1^\pm \tilde{\chi}_1^\pm$  pair production by VBF processes,  $V$ +jets background, and  $VV$  background produced by VBF processes. These distributions show that requiring  $\cancel{E}_T > 75$  GeV is effective in reducing the background.

A summary of the effective cross-section at each selection stage of the study is presented in Table I for the main sources of background and inclusive  $\tilde{\chi}_1^\pm \tilde{\chi}_1^\pm$ ,  $\tilde{\chi}_1^+ \tilde{\chi}_1^-$ ,  $\tilde{\chi}_1^\pm \tilde{\chi}_2^0$  and  $\tilde{\chi}_2^0 \tilde{\chi}_2^0$  pair production by VBF processes. The VBF and  $\cancel{E}_T$  cuts are very effective in reducing the background. The significance (at  $25 \text{ fb}^{-1}$ ) for inclusive, opposite-sign, and like-sign  $\tau$  pairs are 2.4, 1.8, and 1.7, respectively at the benchmark point, where  $\Delta M =$

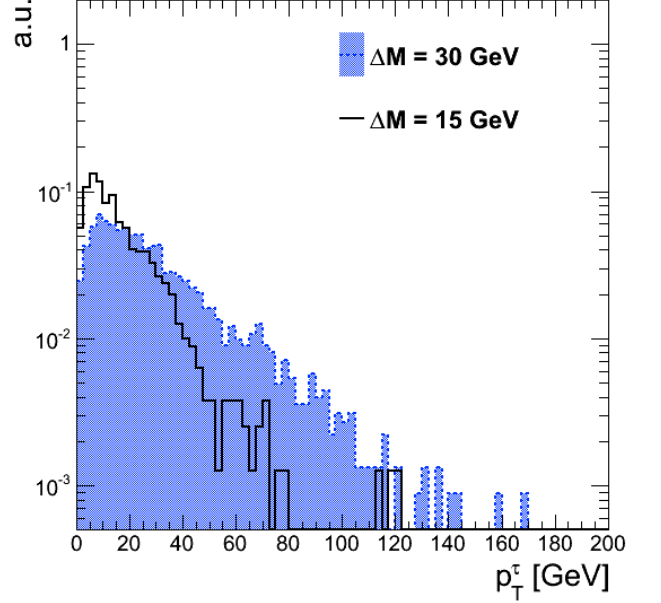


FIG. 5:  $p_T$  of  $\tau$  distribution normalized to arbitrary units in  $\geq 2j + 2\tau$  final state for  $\Delta M = m_{\tilde{\chi}_1^\pm} - m_{\tilde{\chi}_1^0} = 30$  GeV and 15 GeV.

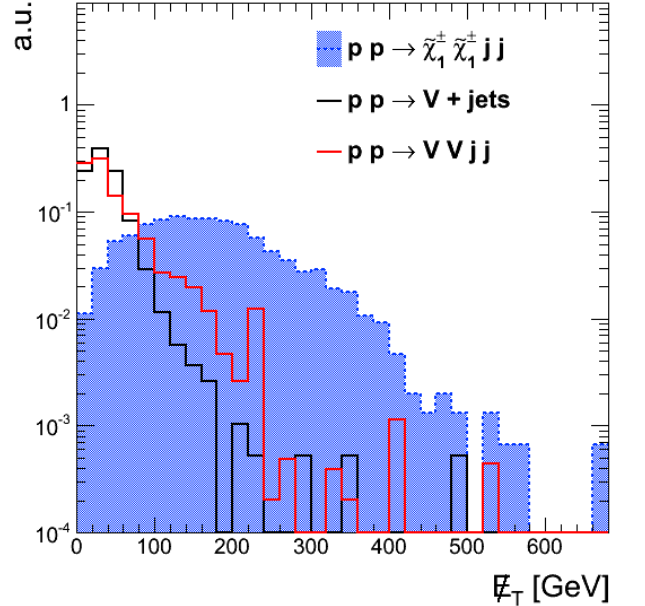


FIG. 6:  $\cancel{E}_T$  distribution normalized to arbitrary units for  $\tilde{\chi}_1^\pm \tilde{\chi}_1^\pm$  pair production by VBF processes,  $V$ +jets background, and  $VV$  background produced by VBF processes.

$m_{\tilde{\tau}_1} - m_{\tilde{\chi}_1^0} = 30$  GeV. For  $\Delta M = 15$  GeV, the significance (at  $25 \text{ fb}^{-1}$ ) for inclusive, opposite-sign, and like-sign  $\tau$  pairs are 0.9, 0.7, and 0.6, respectively.

We have also considered the  $t\bar{t}$  background (cross-section  $225 \text{ fb}$ ) and found that the cross-section for



$\geq 2j + 2\tau$  final state is 0.002 fb (the VBF cut efficiency is  $10^{-3}$ , and the combined efficiency of  $\cancel{E}_T$ ,  $2\tau$  inclusive selection and loose  $b$ -veto is  $\sim 10^{-5}$ ) which is small compared to the other backgrounds. The VBF cuts are very effective in reducing the background in this case unlike the VBF production of Higgs [28, 29] where much lower jet  $p_T$  ( $p_T > 25$  GeV for ATLAS,  $p_T > 30$  GeV for CMS) is used for VBF selection. Also,  $M_{j_1 j_2}$  is much smaller in the VBF production of Higgs (for example CMS used  $M_{j_1 j_2} > 450$  GeV). In the SUSY case, due to the requirement of larger energy in the VBF system to produce chargino/neutralino pair, the jet  $p_T$  is higher which is utilized to select the signal events [15].

Figure 7 shows the distribution of  $M_{j_1 j_2}$  for inclusive  $\tilde{\chi}_1^\pm \tilde{\chi}_1^\pm, \tilde{\chi}_1^\pm \tilde{\chi}_1^\mp, \tilde{\chi}_1^\pm \tilde{\chi}_2^0$  and  $\tilde{\chi}_2^0 \tilde{\chi}_2^0$  pair production by VBF processes and the main sources of background at  $\sqrt{s} = 8$  TeV for 25 fb $^{-1}$  of integrated luminosity. There is an excess of signal over background above  $M_{j_1 j_2} \sim 650$  GeV.

TABLE I: Summary of the effective cross section (fb) for inclusive  $\tilde{\chi}_1^\pm \tilde{\chi}_1^\pm, \tilde{\chi}_1^\pm \tilde{\chi}_1^\mp, \tilde{\chi}_1^\pm \tilde{\chi}_2^0$  and  $\tilde{\chi}_2^0 \tilde{\chi}_2^0$  pair production by VBF processes and main backgrounds in the  $\geq 2j + 2\tau$  final state at  $\sqrt{s} = 8$  TeV. Results for same-sign and oppositely-signed final state  $\tau$  pair, as well as inclusive study, are shown. The final  $t\bar{t}$  cross-section after all cuts is 0.002 fb in the  $\geq 2j + 2\tau$  (inclusive) final state at  $\sqrt{s} = 8$  TeV, and this has been neglected in the computation of the significance. Masses and momenta are in GeV. The significance is displayed for 25 fb $^{-1}$ .

	Signal	Z+jets	W+jets	WW	WZ
VBF cuts	4.61	10.9	$3.70 \times 10^3$	97.0	19.0
$\cancel{E}_T > 75, b\text{-veto}$	4.33	0.27	$5.29 \times 10^2$	17.6	3.45
$2\tau$ , inclusive	0.45	0.06	0.23	0.09	0.04
$(S/\sqrt{S+B})$			2.4		
$\tau^\pm \tau^\pm$	0.21	0	0.11	0.02	0.01
$(S/\sqrt{S+B})$			1.8		
$\tau^\pm \tau^\mp$	0.24	0.06	0.12	0.07	0.03
$(S/\sqrt{S+B})$			1.7		

### B. $\geq 2j + 2\mu + \cancel{E}_T$

In the previous section, the VBF search strategy in the multi- $\tau$  final state has been outlined. Although the search with  $\tau$  leptons are expected to be the most daunting case amongst the three generation of leptons, it is worthwhile to study the potential sensitivity in cases where the charginos and neutralinos preferentially decay to the first two generation of sleptons.

In this subsection, results for event selection with  $\geq 2j + 2\mu + \cancel{E}_T$  are presented. A branching ratio of 100% of  $\tilde{\chi}_1^\pm$  and  $\tilde{\chi}_2^0$  to  $\tilde{\mu}$  has been assumed. After VBF selections, the following selections are employed:

(i) Two isolated  $\mu$ 's with  $p_T \geq 20$  GeV and  $p_T \geq 15$  GeV in  $|\eta| < 2.1$ .

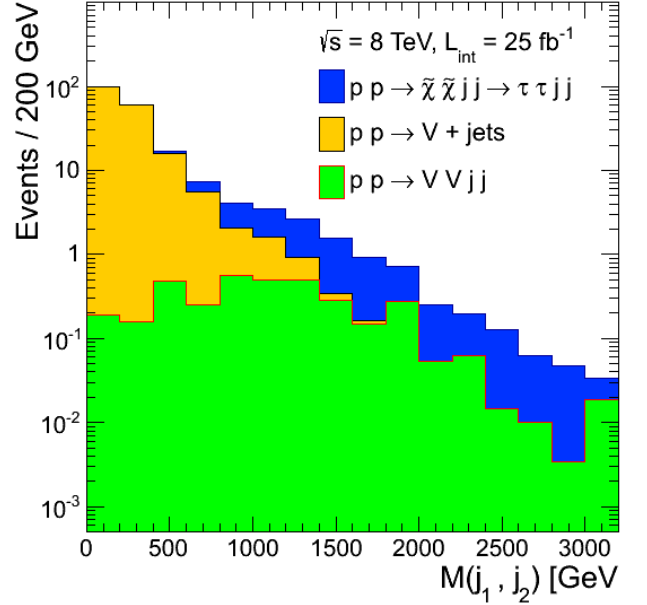


FIG. 7: Distribution of  $M_{j_1 j_2}$  for signal and background at  $\sqrt{s} = 8$  TeV for 25 fb $^{-1}$  of integrated luminosity in the  $\geq 2j + 2\tau$  (inclusive) final state. The blue (dark) region displays  $M_{j_1 j_2}$  distribution for inclusive  $\tilde{\chi}_1^\pm \tilde{\chi}_1^\pm, \tilde{\chi}_1^\pm \tilde{\chi}_1^\mp, \tilde{\chi}_1^\pm \tilde{\chi}_2^0$  and  $\tilde{\chi}_2^0 \tilde{\chi}_2^0$  pair production by VBF processes. The yellow (lightest) region displays  $V$ +jets background. The green (light) region displays  $VV$  background produced by VBF processes.

(ii)  $\cancel{E}_T > 75$  GeV.

(iii) We also apply a loose  $b$ -veto which is useful in reducing the  $t\bar{t}$  background.

A summary of the effective cross-section at each selection stage of the study is presented in Table II for the main sources of background and inclusive  $\tilde{\chi}_1^\pm \tilde{\chi}_1^\pm, \tilde{\chi}_1^\pm \tilde{\chi}_1^\mp, \tilde{\chi}_1^\pm \tilde{\chi}_2^0$  and  $\tilde{\chi}_2^0 \tilde{\chi}_2^0$  pair production by VBF processes. The VBF and  $\cancel{E}_T$  cuts are very effective in reducing the background. The  $t\bar{t}$  background cross-section for  $\geq 2j + 2\mu$  final state is 0.04 fb (the VBF cut efficiency is  $10^{-3}$ , and the combined efficiency of  $\cancel{E}_T$  cut,  $2\mu$  inclusive event selection, and loose  $b$ -veto is  $\sim 2 \times 10^{-4}$ ) which is small compared to the other backgrounds. Also we note that, the inclusive and opposite sign muon cross-sections are same, 0.04 fb, but the same sign dimuon cross-section is almost zero.

The significances (at 25 fb $^{-1}$ ) for inclusive, opposite sign, and like-sign  $\mu$  pairs are 6.0, 4.4, and 4.1, respectively. For  $m_{\tilde{\chi}_1^\pm} \sim m_{\tilde{\chi}_2^0} \sim 260$  GeV, the significances (given by  $S/\sqrt{S+B}$ ) for inclusive, opposite-sign, and like-sign  $\mu$  pairs are approximately 2.7, 1.8, and 1.7, respectively (at 25 fb $^{-1}$ ).

Figure 8 shows the distribution of  $M_{j_1 j_2}$  for inclusive  $\tilde{\chi}_1^\pm \tilde{\chi}_1^\pm, \tilde{\chi}_1^\pm \tilde{\chi}_1^\mp, \tilde{\chi}_1^\pm \tilde{\chi}_2^0$  and  $\tilde{\chi}_2^0 \tilde{\chi}_2^0$  pair production by VBF processes and main sources of background at  $\sqrt{s} = 8$  TeV for 25 fb $^{-1}$  of integrated luminosity. There is an excess of signal over background above  $M_{j_1 j_2} \sim 650$  GeV.

TABLE II: Summary of the effective cross section (fb) for inclusive  $\tilde{\chi}_1^\pm \tilde{\chi}_1^\pm$ ,  $\tilde{\chi}_1^\pm \tilde{\chi}_1^\mp$ ,  $\tilde{\chi}_1^\pm \tilde{\chi}_2^0$  and  $\tilde{\chi}_2^0 \tilde{\chi}_2^0$  pair production by VBF processes and main backgrounds in the  $\geq 2j + 2\mu$  final state at  $\sqrt{s} = 8$  TeV. Results for same-sign and oppositely-signed final state  $\mu$  pair, as well as inclusive study, are shown. The final  $t\bar{t}$  cross-section after all cuts is 0.04 fb in the  $\geq 2j + 2\mu$  (inclusive) final state at  $\sqrt{s} = 8$  TeV, and this has been added in the computation of the significance (inclusive and opposite sign muon cross-sections are same, 0.04 fb, but the same sign dimuon cross-section is almost zero). Masses and momenta are in GeV. The significance is displayed for  $25 \text{ fb}^{-1}$ .

	Signal	$Z$ +jets	$W$ +jets	$WW$	$WZ$
VBF cuts	4.61	10.9	$3.70 \times 10^3$	97.0	19.0
$\cancel{E}_T > 75$	4.33	0.27	$5.29 \times 10^2$	17.6	3.45
$2\mu$ , inclusive	1.83	0.15	0	0.12	0.19
$(S/\sqrt{S+B})$			6.0		
$\mu^\pm \mu^\pm$	0.87	0	0	0.03	0.05
$(S/\sqrt{S+B})$			4.5		
$\mu^\pm \mu^\mp$	0.96	0.15	0	0.09	0.14
$(S/\sqrt{S+B})$			4.1		

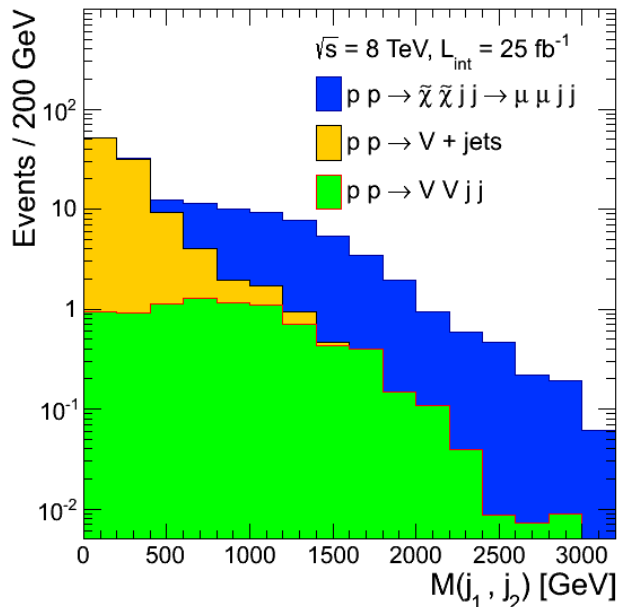


FIG. 8: Distribution of  $M_{j_1 j_2}$  for signal and background at  $\sqrt{s} = 8$  TeV for  $25 \text{ fb}^{-1}$  of integrated luminosity in the  $\geq 2j + 2\mu$  (inclusive) final state. The blue (dark) region displays  $M_{j_1 j_2}$  distribution for inclusive  $\tilde{\chi}_1^\pm \tilde{\chi}_1^\pm$ ,  $\tilde{\chi}_1^\pm \tilde{\chi}_1^\mp$ ,  $\tilde{\chi}_1^\pm \tilde{\chi}_2^0$  and  $\tilde{\chi}_2^0 \tilde{\chi}_2^0$  pair production by VBF processes. The yellow (lightest) region displays  $V$ + jets background. The green (light) region displays  $VV$  background produced by VBF processes.

## IV. CONCLUSION

This paper has investigated the production of  $\tilde{\chi}_1^\pm$  and  $\tilde{\chi}_2^0$  by VBF processes at the LHC at  $\sqrt{s} = 8$  TeV. The presence of high  $E_T$  forward jets in opposite hemispheres with large dijet invariant mass is used to identify the VBF production. Kinematic requirements to search for signals of these supersymmetric particles above SM background arising from VBF and non-VBF processes have been developed. They have been shown to be effective in searching for  $\tilde{\chi}_1^\pm$  and  $\tilde{\chi}_2^0$  in both  $2l$  as well as  $2\tau$  final states.

Searches for the EW sector in  $\tau$  final states in Drell-Yan production face the challenge of controlling the level of backgrounds due to the larger  $\tau$  misidentification rate as well as maintaining low enough  $p_T$  thresholds for triggering. The VBF searches are capable of reducing the background to manageable levels and thus probing multi- $\tau$  final states.

At the benchmark point ( $m_{\tilde{\chi}_1^\pm} \sim m_{\tilde{\chi}_2^0} = 181$  GeV,  $m_{\tilde{\tau}_1} = 130$  GeV, and  $m_{\tilde{\chi}_1^0} = 100$  GeV), the significances (at  $25 \text{ fb}^{-1}$ ) for inclusive, opposite-sign, and like-sign  $\tau$  pairs are 2.4, 1.8, and 1.7, respectively, for  $\Delta M = m_{\tilde{\tau}_1} - m_{\tilde{\chi}_1^0} = 30$  GeV, while 0.9, 0.7 and 0.6, respectively, for  $\Delta M = 15$  GeV.

The significances for inclusive, opposite-sign, and like-sign  $\mu$  pairs are 6.0, 4.5, and 4.1, respectively, at the benchmark point. However, the significances are reduced to 2.7, 1.8, and 1.7, respectively, for  $m_{\tilde{\chi}_1^\pm} \sim m_{\tilde{\chi}_2^0} \sim 260$  GeV.

The next-to-leading order QCD corrections to the VBF electroweak production cross sections have not been considered. The inclusion of the K factor, which is very modest for VBF production ( $\sim 5\%$ ) [29], would improve the signal significance [30].

With increasing instantaneous luminosity, both ATLAS and CMS experiments are raising their  $p_T$  thresholds for triggering objects. The VBF trigger offers a promising route to probe supersymmetric production free from trigger bias. This is complementary to the existing LHC searches based on Drell-Yan production.

## V. ACKNOWLEDGMENTS

We would like to thank Sean Wu for useful discussions. This work is supported in part by the DOE grant DE-FG02-95ER40917, by the World Class University (WCU) project through the National Research Foundation (NRF) of Korea funded by the Ministry of Education, Science & Technology (grant No. R32-2008-000-20001-0), and by the National Science Foundation grant PHY-1206044.

[1] ATLAS Collaboration, “Search for squarks and gluinos with the ATLAS detector in final states with jets and

missing transverse momentum using  $4.7 \text{ fb}^{-1}$  of  $\sqrt{s} = 7$

- TeV proton-proton collision data,” arXiv:1208.0949 [hep-ex].
- [2] ATLAS Collaboration, “Hunt for new phenomena using large jet multiplicities and missing transverse momentum with ATLAS in  $4.7 \text{ fb}^{-1}$  of  $\sqrt{s} = 7 \text{ TeV}$  proton-proton collisions,” JHEP **07**, 167 (2012) [arXiv:1206.1760 [hep-ex]].
- [3] CMS Collaboration, “Search for new physics in the multijet and missing transverse momentum final state in proton-proton collisions at  $\sqrt{s} = 7 \text{ TeV}$ ,” arXiv:1207.1898 [hep-ex].
- [4] B. Dutta, T. Kamon, N. Koley, K. Sinha and K. Wang, “Searching for Top Squarks at the LHC in Fully Hadronic Final State, Phys. Rev. D **86**, 075004 (2012) [arXiv:1207.1873 [hep-ph]].
- [5] T. Plehn and M. Spannowsky, “Top Tagging,” arXiv:1112.4441 [hep-ph]. T. Plehn, M. Spannowsky and M. Takeuchi, “Stop searches in 2012,” arXiv:1205.2696 [hep-ph]. D. E. Kaplan, K. Rehermann and D. Stolarski, “Searching for Direct Stop Production in Hadronic Top Data at the LHC,” arXiv:1205.5816 [hep-ph]. D. S. M. Alves, M. R. Buckley, P. J. Fox, J. D. Lykken and C. -T. Yu, “Stops and MET: the shape of things to come,” arXiv:1205.5805 [hep-ph]. T. Han, R. Mahbubani, D. G. E. Walker and L. -T. Wang, “Top Quark Pair plus Large Missing Energy at the LHC,” JHEP **05**, 117 (2009) [arXiv:0803.3820 [hep-ph]]. Y. Bai, H. -C. Cheng, J. Gallicchio and J. Gu, “Stop the Top Background of the Stop Search,” JHEP **07**, 110 (2012) [arXiv:1203.4813 [hep-ph]].
- [6] ATLAS Collaboration, “Search for direct top squark pair production in final states with one isolated lepton, jets, and missing transverse momentum in  $\sqrt{s} = 7 \text{ TeV}$  pp collisions using  $4.7 \text{ fb}^{-1}$  of ATLAS data,” ATLAS-CONF-2012-073.
- [7] K. Choi and H. P. Nilles, “The Gaugino code,” JHEP **04**, 006 (2007) [hep-ph/0702146 [HEP-PH]].
- [8] R. Allahverdi, B. Dutta and K. Sinha, “Non-thermal Higgsino Dark Matter: Cosmological Motivations and Implications for a 125 GeV Higgs,” arXiv:1208.0115 [hep-ph].
- [9] R. L. Arnowitz, B. Dutta, A. Gurrola, T. Kamon, A. Krislock and D. Toback, “Determining the Dark Matter Relic Density in the mSUGRA Neutralino-Stau Co-Annihilation Region at the LHC,” Phys. Rev. Lett. **100**, 231802 (2008) [arXiv:0802.2968 [hep-ph]].
- [10] I. Hinchliffe, F. E. Paige, M. D. Shapiro, J. Soderqvist and W. Yao, “Precision SUSY measurements at CERN LHC,” Phys. Rev. D **55**, 5520 (1997) [arXiv:hep-ph/9610544]. I. Hinchliffe and F. E. Paige, “Measurements in SUGRA models with large  $\tan(\beta)$  at LHC,” Phys. Rev. D **61**, 095011 (2000) [arXiv:hep-ph/9907519].
- [11] B. Dutta, T. Kamon, A. Krislock, K. Sinha and K. Wang, “Diagnosis of Supersymmetry Breaking Mediation Schemes by Mass Reconstruction at the LHC,” Phys. Rev. D **85**, 115007 (2012) [arXiv:1112.3966 [hep-ph]].
- [12] R. N. Cahn and S. Dawson, “Production of Very Massive Higgs Bosons,” Phys. Lett. B **136**, 196 (1984) [Erratum-ibid. B **138**, 464 (1984)].
- [13] J. D. Bjorken, “Rapidity gaps and jets as a new physics signature in very high-energy hadron hadron collisions,” Phys. Rev. D **47**, 101 (1993).
- [14] D. L. Rainwater, D. Zeppenfeld and K. Hagiwara, “Searching for  $H \rightarrow \tau^+ \tau^-$  in weak boson fusion at the CERN LHC,” Phys. Rev. D **59**, 014037 (1998) [hep-ph/9808468].
- [15] D. Choudhury, A. Datta, K. Huitu, P. Konar, S. Moretti and B. Mukhopadhyaya, “Slepton production from gauge boson fusion,” Phys. Rev. D **68**, 075007 (2003) [hep-ph/0304192]. A. Datta and K. Huitu, “Characteristic slepton signal in anomaly mediated SUSY breaking models via gauge boson fusion at the CERN LHC,” Phys. Rev. D **67**, 115006 (2003) [hep-ph/0211319].
- [16] G. -C. Cho, K. Hagiwara, J. Kanzaki, T. Plehn, D. Rainwater and T. Stelzer, “Weak boson fusion production of supersymmetric particles at the CERN LHC,” Phys. Rev. D **73**, 054002 (2006) [hep-ph/0601063].
- [17] A. Datta, P. Konar and B. Mukhopadhyaya, “Signals of neutralinos and charginos from gauge boson fusion at the Large Hadron Collider,” Phys. Rev. D **65**, 055008 (2002) [hep-ph/0109071]; “Invisible charginos and neutralinos from gauge boson fusion: A Way to explore anomaly mediation?,” Phys. Rev. Lett. **88**, 181802 (2002) [hep-ph/0111012]; P. Konar and B. Mukhopadhyaya, “Gauge boson fusion as a probe of inverted hierarchies in supersymmetry,” Phys. Rev. D **70**, 115011 (2004) [hep-ph/0311347].
- [18] ATLAS Collaboration, “Search for direct production of charginos and neutralinos in events with three leptons and missing transverse momentum in  $\sqrt{s} = 7 \text{ TeV}$   $pp$  collisions with the ATLAS detector,” ATLAS-CONF-2012-077.
- [19] ATLAS Collaboration, “Search for anomaly-mediated supersymmetry breaking with the ATLAS detector based on a disappearing-track signature in  $pp$  collisions at  $\sqrt{s} = 7 \text{ TeV}$ ,” Eur. Phys. J. C **72**, 1993 (2012) [arXiv:1202.4847 [hep-ex]].
- [20] CMS Collaboration, “Search for anomalous production of multilepton events in  $pp$  collisions at  $\sqrt{s} = 7 \text{ TeV}$ ,” JHEP **06**, 169 (2012) [arXiv:1204.5341 [hep-ex]].
- [21] K. Griest and D. Seckel, “Three exceptions in the calculation of relic abundances,” Phys. Rev. D **43**, 3191 (1991).
- [22] M. Carena, S. Gori, N. R. Shah and C. E. M. Wagner, “A 125 GeV SM-like Higgs in the MSSM and the  $\gamma\gamma$  rate,” JHEP **03**, 014 (2012) [arXiv:1112.3336 [hep-ph]].
- [23] J. Alwall, “MadGraph/MadEvent v4: the new web generation,” JHEP **09**, 028 (2008) [arXiv:0706.2334 [hep-ph]].
- [24] PGS4 is a parameterized detector simulator. We use version 4 (<http://www.physics.ucdavis.edu/~conway/research/software/pgs/pgs4-general.htm>) in the LHC detector configuration. The  $b$ -jet tagging efficiency in PGS is  $\sim 42\%$  for  $E_T > 50 \text{ GeV}$  and  $|\eta| < 1.0$ , and degrading between  $1.0 < |\eta| < 1.5$ . The  $b$ -tagging fake rate for  $c$  and light quarks/gluons is  $\sim 9\%$  and  $2\%$ , respectively. So far, no problem has been reported to carry out 8 TeV in any analyses.
- [25] CMS Collaboration, “Measurement of the electroweak production cross section of the  $Z$  boson with two forward-backward jets in  $pp$  collisions at 7 TeV, CMS-PAS-FSQ-12-019.
- [26] ATLAS collaboration, “Jet energy measurement with the ATLAS detector in proton-proton collisions at  $\sqrt{s} = 7 \text{ TeV}$ ,” arXiv:1112.6426.
- [27] CMS Collaboration, “Performance of  $\tau$ -lepton reconstruction and identification in CMS, J. Instrum. **07** P01001 (2012), doi:10.1088/1748-0221/7/01/P01001.
- [28] CMS Collaboration, “Search for the standard model



- Higgs boson decaying to  $W^+W$  in the fully leptonic final state in  $pp$  collisions at  $\sqrt{s} = 8$  TeV,” CMS-PAS-HIG-12-038.
- [29] ATLAS Collaboration, “Search for the Standard Model Higgs boson in the  $H \rightarrow WW(*) \rightarrow \ell\nu\ell\nu$  decay mode with  $4.7 \text{ fb}^{-1}$  of ATLAS data at  $\sqrt{s} = 7$  TeV,” Phys. Lett. B **716**, 62 (2012) [arXiv:1206.0756 [hep-ex]].
- [30] T. Figy, C. Oleari and D. Zeppenfeld, “Next-to-leading order jet distributions for Higgs boson production via weak boson fusion,” Phys. Rev. D **68**, 073005 (2003) [hep-ph/0306109]; P. Konar and D. Zeppenfeld, “Next-to-leading order QCD corrections to slepton pair production via vector-boson fusion,” Phys. Lett. B **647**, 460 (2007) [hep-ph/0612119]; C. Oleari and D. Zeppenfeld, Phys. Rev. D **69**, 093004 (2004) [hep-ph/0310156].